Optimization of Small-Hole Drilling Parameters in Electrical Discharge Machining Using Grey Relational Analysis

Tavee Madsa
Faculty of Engineering, Rajamangala University of Technology Krungthep, Nanglinchee, Thungmahamek, Sathon, Bangkok, Thailand
tavee.m_dd@mail.rmutk.ac.th

Kamonpong Jamkamon
Faculty of Engineering, Rajamangala University of Technology Krungthep, Nanglinchee, Thungmahamek, Sathon, Bangkok, Thailand
kamonpong.j@mail.rmutk.ac.th (corresponding author)

Received: 28 December 2025 | Revised: 31 January 2026 | Accepted: 8 February 2026

 DOI: https://doi.org/10.48084/etasr.17211

ABSTRACT

This study presents an optimization technique for the machining conditions of the small-hole Electrical Discharge Machining (EDM) drilling process. Performance characteristics, such as the Material Removal Rate (MRR) and Electrode Wear Ratio (EWR), were evaluated using Grey Relational Analysis (GRA). A One-Factor-At-a-Time (OFAT) experimental design was employed for testing on SKD61 tool steel, with a brass tube tool electrode of 1 mm outer diameter . The control machining conditions consisted of discharge current, pulse-on time, and pulse-off time. Multiresponse optimization was identified with GRA at a discharge current of 25.5 A, a pulse-on time of 70 µs, and a pulse-off time of 10 µs. The Grey Relational Grade (GRG) improved by approximately 23.79%. The mean MRR and EWR were 5.3484 mm³/min and 2.3139 mm³/min with prediction errors of 6.51% and 7.55%, respectively. Scanning Electron Microscopy (SEM) revealed that electrode wear mainly occurred at the corners and end face of the tubular electrode, resulting in a tapered tool tip and, correspondingly, a tapered drilled hole. The findings suggest that applying optimization parameters using OFAT is feasible with the GRA. In addition, the latter constitutes a robust methodology for multiresponse optimization. The study did not employ any specialized commercial software, demonstrating the utility of GRA in a wide range of manufacturing operations.

Keywords-EDM small-hole drilling; SKD61; MRR; EWR; grey relational analysis

I. INTRODUCTION

Small-hole drilling on tool steels is difficult to perform with conventional machining processes because of the high speed of spindle rotation and the difficulty of chip flow out from the cutting area. Small hole drilling by EDM is widely used to produce automotive parts, molds, and dies from difficult-to-cut materials [1] because the noncontact tool electrode and work material can avoid the acting force in the machining process. Most researchers have attempted to overcome the limitations of the machining processes [2]. Authors in [3] modified electrodes to improve the machining performance of small-hole EDM drilling. They reported that the compared with solid round bars, dumbbell-shaped electrodes can be drilled deeper. In addition, the stirrer-shaped electrode could be easily machined up to 8 times the length per diameter. Authors in [4] developed a discharge state based on the frequency detection method. The results revealed that accurately controlling the amplitude of the voltage and current of the discharge stage can increase the machining performance by 22.4% and reduce the burned area of the inner surface of the hole by approximately 38.2%.

In [5], multiple performance characteristics of the EDM process were optimized through hole drilling. A Taguchi L16 orthogonal array was used to evaluate the influence of process parameters on the machining time, average overcut, taper angle, entry overcut, exit overcut, and MRR. The expected outcome obtained at the optimal condition was improved by approximately 10.57% over the grand average of machining performance. In addition, the Analytic Hierarchy Process (AHP) has been applied to predict the performance of EDM parameters, thereby estimating both MRR and surface roughness during the machining of 90CrSi steel. The AHP is a practical and flexible framework for evaluating alternatives, particularly when a limited number of key criteria entail substantial trade-offs [6]. Authors in [7] used Analysis of Variance (ANOVA) and an Artificial Neural Network (ANN) to assess the influence of key EDM parameters, such as current,

pulse-on time, and pulse-off time, on surface roughness and the EWR, with minimum pulse-on and pulse-off times resulting in the optimal surface finish. The ANN model was developed and evaluated using MATLAB software.

Industrial engineers perform OFAT experiment design to examine process improvement and support problem-solving. However, OFAT experiments can be inefficient and unreliable, leading to false optimal conditions [8]. Despite its simplicity, it fails to consider any possible interactions between factors. The OFAT approach is often adopted in laboratories that lack access to specialized software for Design of Experiment (DoE) or have limited personnel trained in DoE methodologies [9]. Thus, OFAT is often chosen instead of the Taguchi or a full factorial design. The former is very effective in scrutinizing the variables in newly developed processes. It is used to optimize the potential parameters for the final experiments and the effect of each OFAT variable is studied while keeping the other parameters constant [10]. The OFAT approach does not accurately reflect real-world scenarios that involve cross-coupling effects of the parameters, as it assumes black-or-white situations with either complete information or no information. In real-world scenarios, most problems are characterized by shades of grey, where parameters interact, and multiple objectives must be fulfilled. When a problem must provide multiple responses, the parameters are optimized using GRA [11].

The machining performance of small-hole EDM drilling has been experimentally improved with varied solutions. Modified electrodes [3] and improved systems for controlling electrical sparking [4] have been proposed; however, choosing the appropriate method for solving multiple-result problems is important. Moreover, an optimized condition for the DoEs has been analyzed using OFAT. The novelty of the present study lies in the use of GRA to predict the optimal conditions for multiple responses on OFAT. The machining process involved small-hole EDM drilling, with controlled discharge current, pulse-on time, and pulse-off time to predict the multiple responses of the MRR and EWR. The prediction error and experimental tests were employed to evaluate the feasibility of the proposed method.

II. EXPERIMENTAL DETAILS

A. Materials and Methods

The experimental tests were conducted using Koton KTH-200, a small-hole EDM drilling machine, with a precise vise fixed on the table of the machine, as shown in Figure 1. The tool steel of SKD61 grade was used as the workpiece for through-hole drilling with a machining depth of 20 mm. A brass tube electrode of 1 mm outer diameter was employed. Drilling was performed with the dielectric flushing fluid of deionized water. A Tektronix TBS 1000C oscilloscope was used to detect and record the signal of an electrical spark. The machining time (T) was directly recorded by a stopwatch. The weights of the workpiece and electrode before and after machining were measured by a digital balance to evaluate the performance in terms of the MRR and EWR.

Fig. 1. Experimental setup for small-hole EDM drilling.

B. Machining Conditions

The experiments were conducted with controlled machining parameters such as discharge current (I_p), pulse-on time (T_{on}), and pulse-off time (T_{off}), as presented in Table I. A total of 26 experimental runs were conducted following an OFAT design strategy. Each experiment was repeated three times to reduce variability in the experimental tests, and the average values were recorded as testing results. The MRR and EWR can be calculated using:

$$MRR = \frac{W_{iw} - W_{fw}}{T \cdot \rho_w} \quad (1)$$

$$EWR = \frac{W_{eb} - W_{ea}}{T \cdot \rho_e} \quad (2)$$

where W_{iw} and W_{fw} are the weights (g) of the workpiece before and after machining, respectively, and W_{eb} and W_{ea} are the weights (g) of the electrode before and after machining, respectively. T represents the machining time in min, and ρ_w and ρ_e are the densities of the workpiece (0.007855 g/mm^3) and electrode (0.00873 g/mm^3), respectively.

TABLE I. MACHINING PARAMETERS

Parameters (unit)	Symbol	Details
Current (A)	I_P	7.5, 10.5, 13.5, 18.0, 19.5, 21.0, 23.5, 25.5
Pulse-on time (μs)	T_{on}	28, 37, 47, 59, 70, 78, 90, 94, 109
Pulse-off time (μs)	T_{off}	10, 13, 25, 40, 50, 55, 69, 73, 87
Voltage (V)	-	18~22
Dielectric pressure (kg/cm^2)	-	75

C. Grey Relational Analysis

GRA for multiresponse optimization was performed with multiple steps, including problem definition, data normalization, determination of the Grey Relational Coefficient (GRC) and GRG, selection of appropriate variables, and result validation [12, 13]. The influences of I_p, T_{on}, and T_{off} on the MRR and EWR were normalized to grades of 0 to 1, while a GRC weight of 0.5 was given to both MRR and EWR. The GRG was evaluated by calculating the mean of the combination of MRR and EWR in terms of the GRC, after

which the mean GRG of each machining parameter for a given level was determined. Finally, the appropriate variable factors for the optimized condition with the highest GRG for each machining parameter were selected to predict the response, and the errors were compared with those of the experimental test.

III. RESULTS AND DISCUSSION

A. Experimental Results

Testing was conducted by varying I_p, while T_{on} and T_{off} were kept constant at 70 µs and 50 µs, respectively. At an I_p of 25.5 A, the MRR reached a maximum value of 4.7751 ± 0.1818 mm³/min, whereas the corresponding EWR was 1.7267 ± 0.0482 mm³/min. In contrast, when I_p was reduced to 7.5 A, the MRR and EWR decreased to their minimum values of 2.1054 ± 0.1020 mm³/min and 0.6219 ± 0.0045 mm³/min, respectively. The Standard Deviation (SD) for the MRR and EWR ranged from 0.0024 to 0.1818 and 0.0022 to 0.0497, respectively. The experimental MRR and EWR are presented in Table II. The raw data for the experimental results were processed using GRA for a normalized range of 0 to 1. A higher MRR and a lower EWR are desirable. The larger-the-better and smaller-the-better criteria were adopted for MRR and EWR according to:

$$X_i^*(k) = \frac{X_i^{(0)}(k) - min_{all(i)} X_i^{(0)}(k)}{max_{all(i)} X_i^{(0)}(k) - min_{all(i)} X_i^{(0)}(k)} \quad (3)$$

$$X_i^*(k) = \frac{max_{all(i)} X_i^{(0)}(k) - X_i^{(0)}(k)}{max_{all(i)} X_i^{(0)}(k) - min_{all(i)} X_i^{(0)}(k)} \quad (4)$$

where $X_i^*(k)$ is the normalized value of the i^{th} alternative for the k response, $min_{all(i)} X_i^{(0)}(k)$ is the smallest value of $X_i^{(0)}(k)$ for the k response, and $max_{all(i)} X_i^{(0)}(k)$ is the largest value of the corresponding raw experimental data. The $X_i^{(0)}(k)$ terms represent the original experimental value of the k response. The normalized values of the MRR and EWR are presented in Table III.

As shown in Table III, the minimum MRR is 2.1054 mm³/min, corresponding to a normalized value of 0.0000, whereas the maximum MRR is 4.7751 mm³/min, corresponding to a normalized value of 1.0000. The EWRs of 0.6219 mm³/min (minimum) and 1.7444 mm³/min (maximum) were normalized to 1.0000 and 0.0000, respectively. Thus, the lowest electrode wear rate represents the highest performance of the machining process. The GRC is mathematically expressed in (5). It is calculated by considering both the absolute deviation between the normalized value and the reference sequence and the distinguishing coefficient that controls the sensitivity of the analysis. This step is crucial for multiresponse optimization because it enables diverse performance indicators, such as the MRR and EWR, to be evaluated within a unified framework:

$$\xi_i(k) = \frac{\Delta_{min} + \xi \Delta_{max}}{\Delta_{0i}(k) + \xi \Delta_{max}} \quad (5)$$

where Δ_{max} is the maximum value of $\Delta_{0i}(k)$, Δ_{min} is the minimum value of $\Delta_{0i}(k)$, $\xi_i(k)$ is the GRC for the i^{th} performance characteristics, ξ is the distinguishing coefficient, which ranges from 0 to 1, and is generally set to 0.5. The distinguishing coefficient value of 0.5 represents equal weight for both quality characteristics [14, 15]. Finally, the mean GRG value is determined by taking the average of all GRC values.

TABLE II. EXPERIMENTAL MRR AND EWR

I_P (A)	T_{on} (µs)	T_{off} (µs)	MRR (mm³/min)	SD of MRR	EWR (mm³/min)	SD of EWR
7.5	70.0	50.0	2.1054	0.1020	0.6219	0.0045
10.5	70.0	50.0	2.7293	0.0766	0.6635	0.0210
13.5	70.0	50.0	3.0485	0.1567	0.7632	0.0238
18.0	70.0	50.0	3.1415	0.0987	0.9742	0.0049
19.5	70.0	50.0	3.5790	0.0225	1.1965	0.0497
21.0	70.0	50.0	3.6512	0.0590	1.3622	0.0331
23.5	70.0	50.0	3.8582	0.1538	1.5169	0.0068
25.5	70.0	50.0	4.7751	0.1818	1.7267	0.0482
18.0	28.0	50.0	2.4507	0.0105	0.8745	0.0174
18.0	37.0	50.0	2.6225	0.0050	0.9040	0.0276
18.0	47.0	50.0	2.7131	0.0051	0.9686	0.0168
18.0	59.0	50.0	2.7785	0.1112	1.0034	0.0042
18.0	70.0	50.0	3.2089	0.0340	1.0749	0.0230
18.0	78.0	50.0	3.3260	0.0438	1.1833	0.0082
18.0	90.0	50.0	3.4542	0.0838	1.1966	0.0022
18.0	94.0	50.0	3.6030	0.0095	1.4484	0.0093
18.0	109.0	50.0	3.7412	0.0099	1.4613	0.0106
18.0	70.0	10.0	4.5536	0.0069	1.7444	0.0060
18.0	70.0	13.0	3.6510	0.1570	1.5482	0.0251
18.0	70.0	25.0	3.2196	0.1596	1.4724	0.0148
18.0	70.0	40.0	2.9608	0.0094	1.3055	0.0086
18.0	70.0	50.0	2.9104	0.0032	0.9772	0.0167
18.0	70.0	55.0	2.7917	0.0035	0.9410	0.0056
18.0	70.0	69.0	2.3479	0.0248	0.8404	0.0347
18.0	70.0	73.0	2.2527	0.0118	0.7317	0.0244
18.0	70.0	87.0	2.1956	0.0024	0.7307	0.0307

TABLE III. NORMALIZED MRR AND EWR

I_P (A)	T_{on} (µs)	T_{off} (µs)	MRR (mm³/min)	EWR (mm³/min)	MRR (0-1)	EWR (0-1)
7.5	70.0	50.0	2.1054	0.6219	0.0000	1.0000
10.5	70.0	50.0	2.7293	0.6635	0.2337	0.9630
13.5	70.0	50.0	3.0485	0.7632	0.3533	0.8741
18.0	70.0	50.0	3.1415	0.9742	0.3881	0.6861
19.5	70.0	50.0	3.5790	1.1965	0.5520	0.4881
21.0	70.0	50.0	3.6512	1.3622	0.5790	0.3405
23.5	70.0	50.0	3.8582	1.5169	0.6565	0.2027
25.5	70.0	50.0	4.7751	1.7267	1.0000	0.0158
18.0	28.0	50.0	2.4507	0.8745	0.1293	0.7749
18.0	37.0	50.0	2.6225	0.9040	0.1937	0.7487
18.0	47.0	50.0	2.7131	0.9686	0.2276	0.6912
18.0	59.0	50.0	2.7785	1.0034	0.2521	0.6601
18.0	70.0	50.0	3.2089	1.0749	0.4133	0.5964
18.0	78.0	50.0	3.3260	1.1833	0.4572	0.4998
18.0	90.0	50.0	3.4542	1.1966	0.5052	0.4880
18.0	94.0	50.0	3.6030	1.4484	0.5610	0.2637
18.0	109.0	50.0	3.7412	1.4613	0.6127	0.2522
18.0	70.0	10.0	4.5536	1.7444	0.9170	0.0000
18.0	70.0	13.0	3.6510	1.5482	0.5789	0.1748
18.0	70.0	25.0	3.2196	1.4724	0.4174	0.2423
18.0	70.0	40.0	2.9608	1.3055	0.3204	0.3910
18.0	70.0	50.0	2.9104	0.9772	0.3015	0.6835
18.0	70.0	55.0	2.7917	0.9410	0.2571	0.7157
18.0	70.0	69.0	2.3479	0.8404	0.0908	0.8054
18.0	70.0	73.0	2.2527	0.7317	0.0552	0.9022
18.0	70.0	87.0	2.1956	0.7307	0.0338	0.9031

Δ_{min}, Δ_{max}, and $\Delta_{0i}(k)$ are calculated using:

$$\Delta_{min} = \min_{\forall j \in i} \min_{\forall k} \left| x_0^*(k) - x_j^*(k) \right| \quad (6)$$

$$\Delta_{min} = \max_{\forall j \in i} \max_{\forall k} \left| x_0^*(k) - x_j^*(k) \right| \quad (7)$$

$$\Delta_{0i} = (k) = |x_0^*(k) - x_i^*| \quad (8)$$

where $D_{0i}(k)$ represents the absolute deviation between the reference sequence $x_0^*(k)$ and the comparability sequence $x_i^*(k)$.

After the GRCs were obtained, they were averaged to calculate the mean GRC for each machining characteristic. The overall evaluation of multiple performance characteristics is based on the GRG, as defined in:

$$\gamma_i = \frac{1}{n} \sum_{k=0}^{n} \xi_i (k) \quad (9)$$

where γ_i is the GRG for the i^{th} experiment and n is the number of performance characteristics.

The results of the GRG for multiple performance characteristics are presented in Table IV. The combination of optimal parameters included the highest mean GRG, with consisted of the current at level 8 (0.6685), pulse-on time at level 5 (0.5454), and pulse-off time at level 1 (0.5955). These levels of controlled parameters represent the optimal conditions as summarized in Table V. The highest I_p of 25.5 A (level 8) provides the best overall performance, because higher discharge current supplies sufficient energy density for effective material removal while maintaining acceptable electrode wear rates [16]. Due to limitations of the OFAT approach, it is difficult to verify the interaction factors. The results of the ANOVA for the MRR and EWR using the calculated value for the GRG are presented in Table VI. The F-ratio value at 95% CI makes it easier to determine which variables are significant for the responses. The contribution of the I_P variable (65.19%) was the most significant. The least significant variables were T_{off} with a 30.39% contribution, and T_{on}, with a 4.12% contribution, as presented in Table VI. The residual plot of the GRG illustrates the internal consistency within the limits, indicating that the proposed model can produce estimates, as shown in Figure 2. The analysis of the mean GRG values, depicted in Figure 3, reveals GRG, which indicates better machining quality. These results confirm the effective combination of I_p level 8 (25.5 A), T_{on} level 5 (70 µs), and T_{off} level 1 (10 µs), providing clear quantitative guidance for maximizing EDM drilling performance through systematic multiresponse optimization. The generalized model for predicting the MRR and EWR of the OFAT approach over the experimental region is expressed by (10) and (11), respectively. The R^2 values for MRR and EWR regression model are 79.98 and 93.36, respectively.

$$Y_{MRR} = 1.1260 + 0.1153A + 0.01687B - 0.02468C \quad (10)$$

$$Y_{EWR} = 0.1470 + 0.06281\text{A} + 0.00751\text{B} - 0.01352\text{C} \quad (11)$$

where A, B, and C are the discharge current, pulse-on time, and pulse-off time, respectively. The values of Y_{MRR} and Y_{EWR} predicted at the optimal level were 5.0003 mm³/min and 2.1392 mm³/min, respectively, when the input variables A, B, and C were set to 25.5 A, 70 µs, and 10 µs, respectively. However, as presented in Table VII, the experimentally obtained MRR and EWR values were 5.3484 mm³/min and 2.3139 mm³/min, respectively. Therefore, the predicted values of MRR and EWR were approximately 6.51% and 7.55% lower than the experimental values. A separate prediction model for each response was therefore required for the OFAT approach.

TABLE IV. GRC AND AVERAGE GRG VALUES

GRC (MRR)	GRC (EWR)	GRG
0.3333	1.0000	0.6666
0.3948	0.9311	0.6629
0.4360	0.7989	0.6175
0.4497	0.6143	0.5320
0.5274	0.4941	0.5108
0.5429	0.4312	0.4870
0.5928	0.3854	0.4891
1.0000	0.3369	0.6685
0.3648	0.6896	0.5272
0.3828	0.6655	0.5241
0.3930	0.6182	0.5056
0.4007	0.5953	0.4980
0.4601	0.5533	0.5067
0.4795	0.4999	0.4897
0.5026	0.4941	0.4984
0.5325	0.4044	0.4684
0.5635	0.4007	0.4821
0.8577	0.3333	0.5955
0.5429	0.3773	0.4601
0.4618	0.3976	0.4297
0.4239	0.4509	0.4374
0.4172	0.6123	0.5148
0.4023	0.6375	0.5199
0.3548	0.7198	0.5373
0.3461	0.8364	0.5912
0.3410	0.8377	0.5893

TABLE V. MEAN GRG FOR MACHINING PARAMETERS

Machining conditions	Mean GRG with varied parameters		
	Current (A)	Pulse-on time (µs)	Pulse-off time(µs)
Level 1	0.6666	0.5272	0.5955
Level 2	0.6629	0.5241	0.4601
Level 3	0.6175	0.5056	0.4297
Level 4	0.5109	0.4980	0.4374
Level 5	0.5108	0.5454	0.5361
Level 6	0.4870	0.4897	0.5199
Level 7	0.4891	0.4984	0.5373
Level 8	0.6685	0.4684	0.5912
Level 9	-	0.4821	0.5893

After the optimal combination of process parameters is determined, the next step is the improvement of the GRG through a confirmatory experiment. The predicted value of the optimal GRG level can be calculated using:

$$\hat{\gamma} = \gamma_m + \sum_{i=1}^{0} (\bar{\gamma} - \gamma_m) \quad (12)$$

where γ_m is the total mean GRG, $\overline{\gamma}$ is the mean GRG at the optimal level of each parameter, and 0 is the number of significant process parameters. The GRG predicted with (12) was 0.7041 and was compared with the results of the confirmatory experiment, which had a GRG value of 0.5366. The results of the GRG improved by approximately 23.79%, calculated as $(0.7041 - 0.5366)/0.7041) \times 100$.

TABLE VI. ANOVA OF GRG

Source	DF	Seq SS	Adj SS	Adj MS	F-Value	Contribution
I_P	7	0.073932	0.054826	0.007832	46.93	65.19%
T_{on}	8	0.004677	0.003535	0.000442	2.65	4.12%
T_{off}	8	0.034468	0.034468	0.004308	25.81	30.39%
Error	2	0.000334	0.000334	0.000167		0.29%
Total	25	0.113411				100.00%

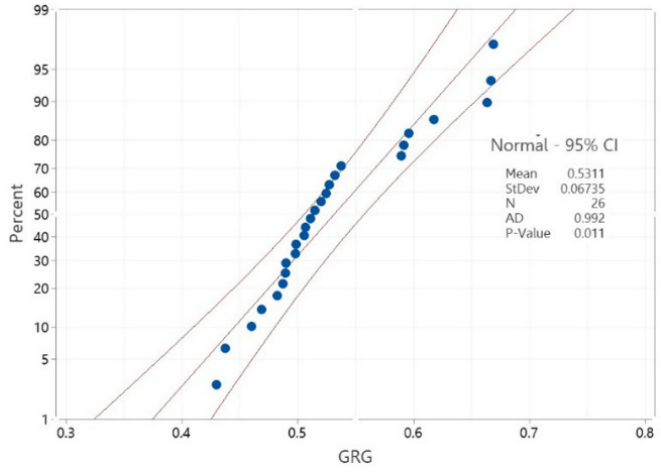

Fig. 2. Confidence intervals and GRG plots.

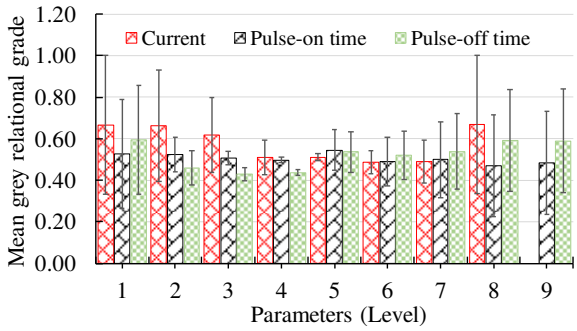

Fig. 3. Mean GRG for the optimal parameter.

TABLE VII. CONFIRMATION OF EXPERIMENTAL RESULTS

No.	I_P (A)	T_{on} (µs)	T_{off} (µs)	MRR (mm^3/min)	EWR (mm^3/min)
1	25.5	70	10	5.2797	2.3898
2	25.5	70	10	5.4802	2.1196
3	25.5	70	10	5.2784	2.2222
4	25.5	70	10	5.2890	2.4615
5	25.5	70	10	5.4148	2.3765
Average				5.3484	2.3139

B. Results of Scanning Electron Microscopy

For further analysis, images of the electrode wear and the wall of the drilled hole were captured using SEM. Figure 4(a-c) shows the SEM images of the hole entrance, mid-depth region, and exit hole, respectively. The entrance region corresponds to the electrode, demonstrating a fine surface of the drilled hole. Higher electrode wear occurred in the middle region of the drilled hole. This wear can be attributed to the limitation of debris particles from the machining area, resulting in a larger area of secondary sparking on the sidewall of the hole and electrode. The electrode experiences the most severe wear at the hole exit region. The tapered tip undergoes extensive melting and pronounced geometric deformation because of the relatively high concentration of discharge energy. The highest wear of the electrode occurred at the end of the brass tube because of the greater density of spark energy. This led to the shortening of the electrode due to thermal erosion caused by an electrical spark. In addition, the high secondary spark at the end of the electrode led to a change in the shape of the brass electrode, which induced a taper on the sidewall of the drilled hole. The diameter at the middle of the drilled hole was larger than the electrode because of the sparking gap induced by the sidewall. Additionally, a small region of secondary sparking can be seen at the hole entrance as the drilled hole was over the side of the electrode. The consumable electrode needed to remove work material per unit time represents the MRR and EWR. In addition, the optimum condition must be met to improve the stability of electrical sparking and machining performance.

C. Spark Signal and Waveform Characteristic Analysis

The electrical spark signal and waveform characteristic for the optimal conditions are shown in Figures 5 and 6, respectively. The current and voltage characteristics of the uniform signal correspond with the duration according to the setup conditions. A T_{on} of 70 µs and a T_{off} of 10 µs represented a sparking cycle. Each cycle of electrical sparking consists of a duration of T_{on} and T_{off} according to the waveform in the EDM process [17, 18]. The discharge duration of electrical sparking at the first stage at high voltage was used to identify the approximate distance between the electrode and the surface of the workpiece, after which the current was applied to eliminate material with the electrical spark. The relationship between the current and the duration of the voltage application indicates that the high voltage is applied without a current-induced gap for the electrical spark in the first stage. Afterward, the voltage was reduced, and the current was increased to achieve a constant electrical spark for the second stage. Finally, both the voltage and the current were reduced to zero during the period of T_{off}. The optimal conditions for a short T_{off} of 10 µs induced continuous electrical sparking. The electrical spark signal and waveform characteristic for low machining performance are presented in Figures 7 and 8. The peak voltage was the highest at the starting cycle of discharge, and the current increased when the gap clearance was approximately equal to that of sparking [4, 19]. A longer T_{off} of 25 µs increased the duration. Therefore, the signal presented a high voltage without current at the first stage. This leads to low machining performance because of the longer stopping period in the circuit of the electrical spark.

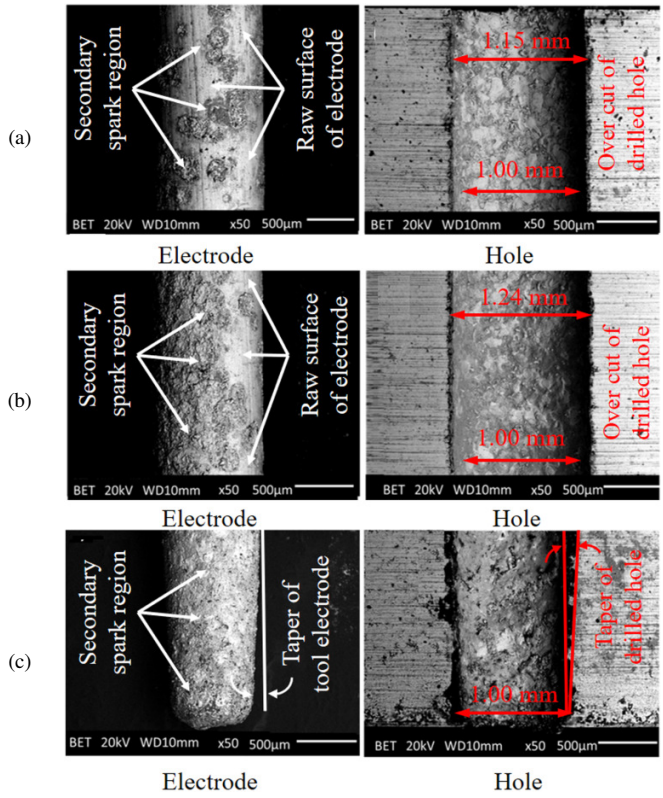

Fig. 4. SEM images of electrode and drilled hole: (a) the hole entrance, (b) the mid-depth region, and (c) the hole exit.

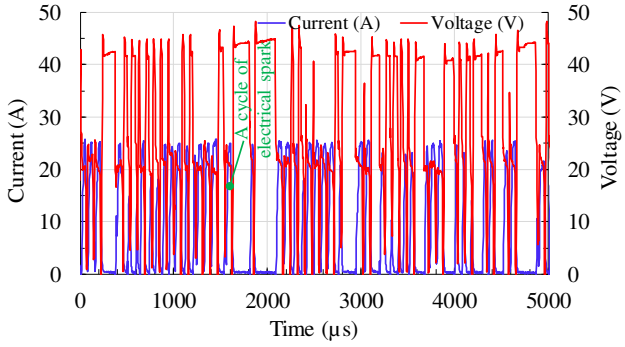

Fig. 5. Signal of the electrical spark under optimal conditions.

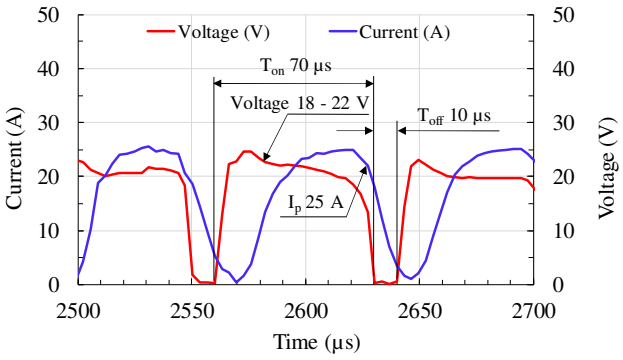

Fig. 6. Characteristics of the waveform at optimal conditions.

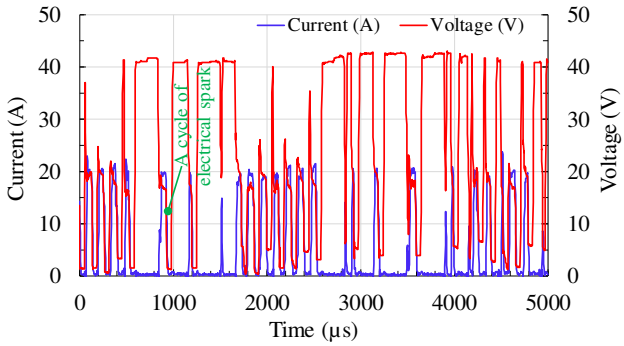

Fig. 7. Signal of the electrical spark at the lowest machining performance.

The quantity of electrical sparks is indicated by the number of stable signals per full sparking cycle according to the calculated value. Under the optimal condition, the signal was maintained a T_{on} of 70 µs and T_{off} of 10 µs for a cycle time of 80 µs. Accordingly, the number of cycles can be estimated as approximately 62.5 cycles (5,000 µs/80 µs). However, electrical sparking occurred for approximately 46.0 cycles, as shown in Figure 5. Therefore, the stability of the electrical spark at the optimal condition was $\left(\frac{46.0}{62.5}\right) \times 100 = 73.6\%$. Similarly, the stability of the electrical spark under the lowest machining conditions was approximately $\left(\frac{26.0}{42.0}\right) \times 100 = 61.90\%$. Electrical sparking occurred for 26 cycles, as illustrated in Figure 7. The calculated number of cycles was 42 ($5000\mu s/(94s + 25\mu s) = 42$). The sparking signal was more stable under optimal conditions.

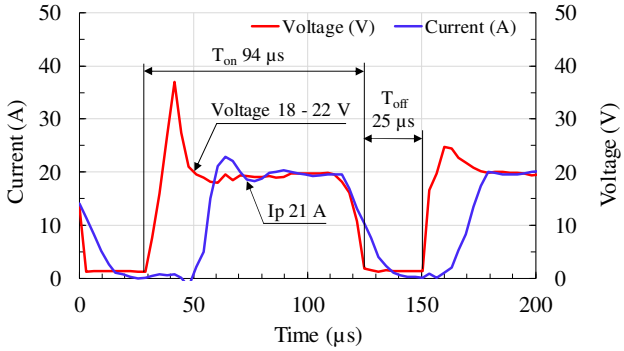

Fig. 8. Characteristics of the waveform of the electrical spark at the lowest machining performance.

IV. CONCLUSIONS

This study investigated the optimal conditions for multiresponse with Grey Relational Analysis (GRA) for small-hole Electrical Discharge Machining (EDM) drilling. The findings of the study are:

- The highest Material Removal Rate (MRR) of the One-Factor-At-a-Time (OFAT) experiment was 4.7751 mm^3/min for an Electrode Wear Ratio (EWR) of 1.7267 mm^3/min. On the other hand, the lowest EWR was 0.6219 mm^3/min with an MRR of 2.1054 mm^3/min. Both the MRR and EWR increased with increasing discharge current (I_p) and pulse-on time (T_{on}).

- The optimal combination of machining parameters was achieved with a discharge current of 25.5 A, T_{on} of 70 µs, and pulse-off time (T_{off}) of 10 µs. The MRR and EWR values predicted were 5.0003 mm³/min and 2.1392 mm³/min, respectively.
- The errors of the predicted values for MRR and EWR were approximately 6.51% and 7.55% lower than the experimental test results, respectively. The optimal Grey Relational Grade (GRG) improved by approximately 23.79%. In addition, the quantitative sparking signal was more stable under the optimal conditions.

The GRA approach is highly effective in analyzing optimal conditions on the basis of the experimental results of OFAT without the need for specific equipment and software. In addition, GRA can be used for predicting optimal conditions according to the OFAT experimental test.

ACKNOWLEDGEMENTS

The authors would like to express their gratitude to the Rajamangala University of Technology Krungthep for financial support and the Rajamangala University of Technology Rattanakosin, Wang Klai Kangwon Campus, for providing laboratory support for this research.

REFERENCES

[1] G. Pellegrini and C. Ravasio, "Study of the Law Motion of the Micro-EDM Drilling Process," *Journal of Manufacturing and Materials Processing*, vol. 7, no. 5, Sept. 2023, Art. no. 165, https://doi.org/10.3390/jmmp7050165.

[2] Y. Sun *et al.*, "Review on Role of Electrical Discharge Drilling Methods in Fabricating Micro Holes: Formation Mechanism, Defects Characterization and Mitigation Strategies," *Archives of Civil and Mechanical Engineering*, vol. 24, no. 3, May 2024, Art. no. 143, https://doi.org/10.1007/s43452-024-00950-5.

[3] A. Hirao, H. Gotoh, and T. Tani, "Effect of Electrode Shape on High Aspect Ratio Deep Hole Drilling by EDM," *Procedia CIRP*, vol. 113, pp. 262–266, 2022, https://doi.org/10.1016/j.procir.2022.09.156.

[4] S. Hou, J. Bai, H. Liu, B. Tian, and Z. Zhou, "Improving Performance of Micro-Hole EDM Based on Frequency Detection Method," *The International Journal of Advanced Manufacturing Technology*, vol. 121, no. 5–6, pp. 3259–3270, July 2022, https://doi.org/10.1007/s00170-022-09560-y.

[5] A. K. Singh, P. K. Patowari, and M. Chandrasekaran, "Experimental Study on Drilling Micro-Hole Through Micro-EDM and Optimization of Multiple Performance Characteristics," *Journal of the Brazilian Society of Mechanical Sciences and Engineering*, vol. 42, no. 10, p. 506, Oct. 2020, https://doi.org/10.1007/s40430-020-02595-w.

[6] F. De Felice, A. Petrillo, and T. Choudhry, *The Art of Decision Making - Applying AHP in Practice*. IntechOpen, 2025.

[7] S. K. Ghazi, M. A. Abdullah, and H. H. Abdulridha, "Investigating the Impact of EDM Parameters on Surface Roughness and Electrode Wear Rate in 7024 Aluminum Alloy," *Engineering, Technology & Applied Science Research*, vol. 15, no. 1, pp. 19401–19407, Feb. 2025, https://doi.org/10.48084/etasr.9252.

[8] J. Antony, T. Chou, and S. Ghosh, "Training for Design of Experiments," *Work Study*, vol. 52, no. 7, pp. 341–346, Dec. 2003, https://doi.org/10.1108/00438020310502642.

[9] M. Mehdizadeh Allaf and C. G. Trick, "Multiple-Stressor Design-of-Experiment (DOE) and One-Factor-At-a-Time (OFAT) Observations Defining Heterosigma Akashiwo Growth and Cell Permeability," *Journal of Applied Phycology*, vol. 31, no. 6, pp. 3515–3526, Dec. 2019, https://doi.org/10.1007/s10811-019-01833-6.

[10] P. Tripathi and S. Singh, "Optimising Parameters for Dry EDM Machining of Inconel 800 Through OFAT Approach," *Defence Science Journal*, vol. 74, no. 6, pp. 937–941, Nov. 2024, https://doi.org/10.14429/dsj.74.19824.

[11] P. Priyalatha, L. Ramayee, R. Kumari, and K. Supradeepan, "Multi-Objective Optimization of a Compact Wideband Antenna Using Grey Relational Analysis," *AEU - International Journal of Electronics and Communications*, vol. 175, Feb. 2024, Art. no. 155063, https://doi.org/10.1016/j.aeue.2023.155063.

[12] K. Mausam, K. Sharma, G. Bharadwaj, and R. P. Singh, "Multi-Objective Optimization Design of Die-Sinking Electric Discharge Machine (EDM) Machining Parameter for CNT-Reinforced Carbon Fibre Nanocomposite Using Grey Relational Analysis," *Journal of the Brazilian Society of Mechanical Sciences and Engineering*, vol. 41, no. 8, Aug. 2019, Art. no. 348, https://doi.org/10.1007/s40430-019-1850-4.

[13] T. T. Nguyen, B. P. Phi, V. T. Tran, V.-T. Nguyen, and V. T. T. Nguyen, "Three-Stage Optimization of Surface Finish in WEDM of D2 Tool Steel via Taguchi Design and ANOVA Analysis," *Metals*, vol. 15, no. 6, June 2025, Art. no. 682, https://doi.org/10.3390/met15060682.

[14] R. Khanna, A. Kumar, M. P. Garg, A. Singh, and N. Sharma, "Multiple Performance Characteristics Optimization for Al 7075 on Electric Discharge Drilling by Taguchi Grey Relational Theory," *Journal of Industrial Engineering International*, vol. 11, no. 4, pp. 459–472, Dec. 2015, https://doi.org/10.1007/s40092-015-0112-z.

[15] V. T. Tran *et al.*, "Optimization Design for Die-Sinking EDM Process Parameters Employing Effective Intelligent Method," *Cogent Engineering*, vol. 10, no. 2, Dec. 2023, Art. no. 2264060, https://doi.org/10.1080/23311916.2023.2264060.

[16] A. P. Tiwary, B. B. Pradhan, and B. Bhattacharyya, "Study on the Influence of Micro-EDM Process Parameters During Machining of Ti–6Al–4V Superalloy," *The International Journal of Advanced Manufacturing Technology*, vol. 76, no. 1–4, pp. 151–160, Jan. 2015, https://doi.org/10.1007/s00170-013-5557-x.

[17] D. Oniszczuk-Świercz and R. Świercz, "EDM – Analyses of Current and Voltage Waveforms," *Mechanik*, no. 2, pp. 112–113, Feb. 2017, https://doi.org/10.17814/mechanik.2017.2.29.

[18] M. Gostimirovic, P. Kovac, B. Skoric, and M. Sekulic, "Effect of Electrical Pulse Parameters on the Machining Performance in EDM," *Indian Journal of Engineering & Materials Sciences*, vol. 18, no. 411–415, Dec. 2012.

[19] F. Caiazzo, L. Cuccaro, I. Fierro, G. Petrone, and V. Alfieri, "Electrical Discharge Machining of René 108 DS Nickel Superalloy for Aerospace Turbine Blades," *Procedia CIRP*, vol. 33, pp. 382–387, 2015, https://doi.org/10.1016/j.procir.2015.06.086.